Study of non-stationary flow of viscoelastic incompressible fluid in a flat channel

Kuralboy Navruzov[1], *Suxrob* Rajabov[2,*], *Nabijon* Abdikarimov[1], *Otabek* Turdimurodov[2], and *Rayhona* Nasrulloeva[2]

[1]Urgench State University, Urgench, Uzbekistan
[2]Kattakurgan branch of Samarkand State University, Samarkand, Uzbekistan

Abstract. The problems of the non-stationary flow of a viscoelastic fluid in a flat channel under the influence of a constant pressure gradient are solved based on the generalized Maxwell model. By solving the problem, formulas for velocity distribution, fluid flow rate, and other hydrodynamic quantities were determined. Based on the formulas derived, transient processes in the unsteady flow of a viscoelastic fluid in a flat channel are analysed. Based on the results of the analysis, it was shown that transient processes depending on the Deborah number, which determines the elasticity property in an elastic-viscous fluid, differ fundamentally from the transient process in a Newtonian fluid. It was discovered that the transition processes of the characteristics of an elastic-viscous fluid from an unsteady to a stationary state at small values of the Deborah number practically do not differ from the transition processes of a Newtonian fluid. At large values of the Deborah number, it was established that the process of transition of an elastic-viscous fluid from an unsteady state to a stationary one is of a wave nature, in contrast to the transition process of a Newtonian fluid, and the transition time is several times longer than the transition time of a Newtonian fluid. It was also revealed that perturbed processes can arise during the transition.

1 Introduction

In many scientific and technological operations, the unsteady flow of a viscoelastic fluid in a flat channel under the effect of a constant pressure gradient is studied. As is known, the viscoelastic properties of non-Newtonian fluids significantly affect the hydrodynamic characteristics of the flow. For example, when transporting highly viscous and heavy oil and petroleum products over long distances and circulating drilling fluid in a well, one of the important tasks is to develop an effective method for reducing the hydrodynamic resistance of flows [1, 2]. In the pipeline transport of viscous and or viscoelastic fluid, an unsteady flow is observed during the starting and stopping modes of the working bodies (mechanismsIn such instances, the fluid flow rate and other hydrodynamic properties of the flow deviate dramatically from those of ordinary Newtonian fluid flows. However, such flows are often employed in different technical processes, including chemical technology, biological

*Corresponding author: rajabovsuxrob72@gmail.com

mechanics, and acoustics. Unsteady flows of Newtonian and non-Newtonian fluids, especially viscoelastic fluids in pipes and channels, have been the subject of several investigations [3–10]. The erratic flow of a viscous incompressible fluid in a cylindrical pipe was initially studied by I.S. Gromeka [3, 4]. He calculated the shear stress on the wall, the velocity change, and the fluid flow rate in these articles. The time of steadying hydrodynamic quantities during the flow of a viscous fluid in a cylindrical conduit may be found using these formulae. Then this problem was studied in [5-10] for unsteady flow of a viscous fluid. In [11], unsteady viscoelastic flows of Oldroyd-B fluid through an infinite pipe of circular cross-section were analyzed. A fluid flows under the influence of a time-dependent pressure gradient in the following three cases: 1) the pressure gradient changes with time by the exponential law; 2) the pressure gradient pulsates; 3) the pressure gradient is constant. Formulas are obtained for the fluid velocity distribution, fluid flow rate, and other hydrodynamic characteristics of the flow.

Unsteady pulsating flows of viscous and viscoelastic fluid in a circular cylindrical pipe of infinite length under the influence of a harmonically changing pressure gradient were studied in [12]. By solving the problem, calculation formulas for the fluid velocity distribution and flow rate were obtained. Numerical calculations have shown that in a pulsating flow at lower values of the dimensionless oscillation frequency, the velocity, flow rate, and other hydrodynamic parameters starting from zero initial state are steadied slowly, compared to high oscillation frequencies and are close to the parameters of a non-pulsating flow. In an oscillating flow at high oscillation frequencies, these parameters are steadied almost instantly. Based on the Maxwell model, the issue of unstable oscillatory flow of a viscoelastic fluid in a flat channel was examined in [13, 14]. Formulas for determining dynamic and frequency characteristics were obtained. The impact of vibration frequency and fluid relaxation characteristics on the shear stress on the wall was investigated by numerical experiments. It is demonstrated that the fluid's acceleration and viscoelastic characteristics are what restrict the use of the quasi-stationary technique. The issues with viscoelastic fluid's erratic flow in long pipes with an annular cross-section were resolved in [15, 16]. Since the fluid's rheological properties were thought to be independent of deformation rate, the issue was simplified to a linear one, and the Laplace transform was used to get an analytical solution.

The computation results were acquired for a Newtonian fluid with constant characteristics, in which the evolution of velocity profiles follows a diffusion-like pattern. At every gap point, the shear stresses and velocity grow monotonically to their stationary values. A fluid's elasticity gives its flow a wave-like quality as it develops. In [17], laminar oscillatory flows of Oldroyd-B and Maxwell viscoelastic fluids were examined; numerous intriguing characteristics that aren't present in Newtonian fluid flows were shown.

In [18], the electro-kinetic flow of viscoelastic fluids in a flat channel under the influence of an oscillatory pressure gradient was studied. It is assumed that the fluid flow is laminar and unidirectional; therefore, the fluid flow has a linear mode. The surface potentials are assumed small, so the Poisson-Boltzmann equation is linearized. During flow, resonant behavior appears when the elastic properties of the Maxwell fluid predominate. The resonance phenomenon enhances electro-kinetic effects, and the efficiency of conversion of electro-kinetic energy is enhanced too.

In the references listed above, the field of fluid velocities is mainly studied under various modes of change in pressure gradient. Inadequate research was done on the variations in the wall's maximum longitudinal velocity, fluid flow rate, and tangential shear stress that happen while an unstable flow moves. In most cases, in hydrodynamic models of unsteady flows, fluids were replaced by a sequence of flows with a quasi-stationary distribution of hydrodynamic quantities. At present, the issue of the validity of studying quasi-stationary characteristics to determine the field of shear stresses in unsteady flows of viscous and viscoelastic fluids has practically not been resolved. Naturally, under such conditions, there is a need to use hydrodynamic models of unsteady processes that take into account changes in the hydrodynamic characteristics of the flow depending on time.

In this article, the authors study the unsteady flow of a viscoelastic fluid using the generalized Maxwell model in a flat channel under the influence of a constant pressure gradient. The distribution of longitudinal velocity, fluid flow rate, and shear stress on the wall are calculated using the following formulas. Transient processes during the starting mode of viscoelastic fluid flow are analyzed.

2 Materials and Methods

Let us consider the problem of unsteady flow of a viscoelastic incompressible fluid between two stationary parallel planes extending in both directions to infinity. We denote the distance between the walls by $2h$. The $0x$-axis runs horizontally in the middle of the channel along the flow. The $0y$-axis is directed perpendicular to the $0x$-axis. The flow of viscoelastic fluid occurs symmetrically along the axis of the channel.

The differential equation of motion of a viscoelastic incompressible fluid under stress has the following form [7-12, 19-23]:

$$\rho\frac{\partial u}{\partial t}=-\frac{\partial p}{\partial x}-\frac{\partial \tau}{\partial y} \tag{1}$$

where u is the longitudinal velocity; p - pressure; ρ - density; τ - shear stress; t -time.

Rheological equations of state of a fluid are taken in the form of a generalized Maxwell equation [17, 18]

$$\tau=\tau_s+\tau_p, \tau_s=-\eta_s\frac{\partial u}{\partial y}, \lambda\frac{\partial \tau_p}{\partial t}+\tau_p=-\eta_p\frac{\partial u}{\partial y} \tag{2}$$

Here λ is the relaxation time; τ_s - shear stress of the Newtonian fluid; τ_p- shear stress of the Maxwell fluid; τ - shear stress of the mixture; η_s - dynamic viscosity of Newtonian fluid; η_p- dynamic viscosity of Maxwell fluid. The equality between dynamic viscosities is satisfied [17, 18, 20, 21]:

$$\eta=\eta_s+\eta_p$$

where η is the dynamic viscosity of the mixture.

Substituting (2) into the equation of motion (1) for the fluid velocity, we obtain:

$$\rho(1+\lambda\frac{\partial}{\partial t})\frac{\partial u}{\partial t}=-(1+\lambda\frac{\partial}{\partial t})\frac{\partial p}{\partial x}+\eta_s(1+\lambda\frac{\partial}{\partial t})\frac{\partial^2 u}{\partial y^2}+\eta_p\frac{\partial^2 u}{\partial y^2} \tag{3}$$

in order to resolve equations (3), The formulation of the initial and boundary conditions is required. Assumedly,
before the time point $t=0$, the fluid is at rest. Starting from $t=0$, the fluid flows because of the pressure gradient's positive constant$\frac{\partial p}{\partial x}=const.$ in this instance, the starting state and the wall's non-slip state will resemble this:

$$u=0 \text{ at } t=0, u=0 \text{ for } y=h \tag{4}$$

In this case, the flow occurs symmetrically along the axis of the channel, therefore

$$\frac{\partial u}{\partial y}=0 \text{ for } y=0\ . \tag{5}$$

Performing the Laplace-Carson transform, i.e. transferring in equation from the original to the picture
(3) and boundary conditions (4) and (5), we obtain:

$$\frac{d^2\bar{u}(y,s)}{dy^2}+\frac{i^2\rho s}{\eta\eta*(s)}\bar{u}(y,s)=\frac{1}{\eta\eta*(s)}\frac{d\bar{p}(x)}{dx} \tag{6}$$

Here $\eta(s) = (\frac{\eta_s}{\eta} + \frac{\eta_p}{\eta}\frac{1}{1+s\lambda}) = (X + Z\frac{1}{1+s\lambda})$, where X and Z are the fractions of Newtonian and Maxwell fluids, respectively [17,18].

Fundamental solutions to the equation without the right-hand side are the functions of cosine and sine $cos\left(i\sqrt{\frac{\rho s}{\eta\eta*(s)}}y\right)$ and $sin\left(i\sqrt{\frac{\rho s}{\eta\eta*(s)}}y\right)$, and partial solution to equation (3) with the right-hand side is constant $-\frac{1}{\rho s}\frac{d\bar{p}(x)}{dx}$.

Thus, the general solution to equation (3) has the following form:

$$\overline{u(y,s)} = C cos\left(i\sqrt{\frac{\rho s}{\eta\eta*(s)}}y\right) + D\, sin\left(i\sqrt{\frac{\rho s}{\eta\eta*(s)}}y\right) - \frac{1}{\rho s}\frac{d\bar{p}(x)}{dx}. \quad (7)$$

Using boundary condition (5), we find constant D, which is equal to zero, and to determine constant C, we use boundary condition (4). As a result, for the velocity image we have:

$$\bar{u}(y,s) = \frac{1}{\rho s}\left(-\frac{d\bar{p}(x)}{dx}\right)\left(1 - \frac{cos\left(i\sqrt{\frac{\rho s}{\eta\eta*(s)}}y\right)}{cos\left(i\sqrt{\frac{\rho s}{\eta\eta*(s)}}h\right)}\right). \quad (8)$$

We derive the integral expression for the fluid velocity as follows using the Laplace-Carson transform's inversion formula:

$$u(y,t) = \frac{1}{2\pi i}\int_{\sigma-i\infty}^{\sigma+i\infty} e^{st}\frac{1}{\rho s}\left(-\frac{dp(x)}{dx}\right)\left(1 - \frac{cos\left(i\sqrt{\frac{\rho s}{\eta\eta*(s)}}y\right)}{cos\left(i\sqrt{\frac{\rho s}{\eta\eta*(s)}}h\right)}\right)\frac{ds}{s} \quad (9)$$

In order to compute the integral (9) over a complex variable, the residues for the integrand must be determined. Given that the roots of the cosine are real integers and that the denominator is equal to zero, we calculate:

$$s = 0 \ \text{ and } \ s = -\nu\frac{s_{1,2,n}}{h^2} \quad (10)$$

Here $s_{1,2,n}$ are the solutions to transcendental equation $cos\left(i\sqrt{\frac{\rho s}{\eta\eta*(s)}}h\right) = 0$. Since there are no complicated poles, we may apply the meromorphic function's expansion into simple fractions in the manner shown below:

$$\frac{F_1(s)}{F_2(s)} = \frac{1}{\rho s}\left(-\frac{dp}{dx}\right)\frac{\left(cos\left(i\sqrt{\frac{\rho s}{\eta\eta*(s)}}h\right) - cos\left(i\sqrt{\frac{\rho s}{\eta\eta*(s)}}y\right)\right)}{cos\left(i\sqrt{\frac{\rho s}{\eta\eta*(s)}}h\right)}\frac{e^{st}}{s} = \frac{C_0}{s} + \sum_{i=1}^{2}\frac{C_{i,n}}{s - s_{i,n}} \quad (11)$$

$$F_1(s) = \left(-\frac{dp}{dx}\right)\left(cos\left(i\sqrt{\frac{\rho s}{\eta\eta*(s)}}h\right) - cos\left(i\sqrt{\frac{\rho s}{\eta\eta*(s)}}y\right)\right)e^{st}; F_2(s) = \rho s^2 cos\left(i\sqrt{\frac{\rho s}{\eta\eta*(s)}}h\right).$$

To determine residue C_0, It is necessary to multiply equality on both sides. (11) by s and then tend s to zero, i.e.

$$C_0 = \lim_{s\to 0}\frac{sF_1(s)}{F_2(s)} = \lim_{s\to 0}\frac{s\left(-\frac{dp}{dx}\right)\left(cos\left(i\sqrt{\frac{\rho s}{\eta\eta*(s)}}h\right) - cos\left(i\sqrt{\frac{\rho s}{\eta\eta*(s)}}y\right)\right)}{\rho s^2 cos\left(i\sqrt{\frac{\rho s}{\eta\eta*(s)}}h\right)} =$$

$$= \frac{1}{2\eta}\left(-\frac{\partial p}{\partial x}\right)h^2\left(1 - \frac{y^2}{h^2}\right). \quad (12)$$

Here, it is assumed that $cos\, x = 1 - \frac{x^2}{2!} + \frac{x^4}{4!} - \cdots$

To determine residue $C_{i,n}$, we need to multiply (11) by the difference $s - s_{in}$ and tend s to s_{in}, considering that

$$C_{in} = \lim_{s\to s_{in}} \frac{F_1(s)}{\frac{F_2(s)-F_2(s_{in})}{s-s_{in}}} = \frac{F_1(s_{in})}{F_2'(s_{in})}. \tag{13}$$

Now we need to find the value of s_{in}, for this, we use equation .$cos\left(i\sqrt{\frac{\rho s}{\eta\eta*(s)}}h\right) = 0.$, its solution has the following form:

$$i\sqrt{\frac{\rho s}{\eta\eta*(s)}}h = \frac{2n+1}{2}\pi \tag{14}$$

Here, considering that $\eta * (s) == (X + Z\frac{1}{1+s\lambda})$, we reduce equation (14) to the following form:

$$\frac{\rho s}{\eta\eta*(s)}h^2 = -\frac{(2n+1)^2}{4}\pi^2 \text{ or } s = -\frac{(2n+1)^2}{4}\pi^2\frac{\nu}{h^2}(X + Z\frac{1}{1+s\lambda}). \tag{15}$$

From here, it is easy to transform equation (15) to the following quadratic equation:

$$De\bar{s}^2 - \bar{s}(1 + XDea_0^2) + a_0^2 = 0 \tag{16}$$

Here $a_0 = \frac{2n+1}{2}\pi,\ De = \frac{\lambda\nu}{h^2},\ s = -\frac{\nu}{h^2}\bar{s}$ There are two roots to quadratic equation (16): real different, real equal, and complex conjugate. We consider all these cases in "Numerical calculations and discussions".

Now, considering that $\bar{s} = s_{in}$,we determine $C_{in} = \lim_{s\to s_{in}} \frac{F_1(\bar{s})}{\frac{F_2(\bar{s})-F_2(s_{in})}{\bar{s}-s_{in}}} = \frac{F_1(s_{in})}{F_2'(s_{in})}$, here, the numerator is easily calculated:

$$F_1(s_{in}) = \left(-\frac{dp}{dx}\right)\left(cos\left(i\sqrt{\frac{\rho s_{in}}{\eta\eta * (s_{in})}}h\right) - cos\left(i\sqrt{\frac{\rho s_{in}}{\eta\eta * (s_{in})}}y\right)\right)e^{s_{in}t} =$$

$$= \left(-\frac{dp}{dx}\right)\left(-cos\left(\frac{(2n+1)}{2}\pi\frac{y}{h}\right)\right)e^{s_{in}t}. \tag{17}$$

Here, it is assumed that $cos\left(i\sqrt{\frac{\rho s_{in}}{\eta\eta*(s_{in})}}h\right) = 0$.

The denominator is calculated using the derivative with respect to s , i.e.

$$F_2{}'(s) = 2\rho s\, cos\left(ih\sqrt{\frac{\rho s}{\eta\eta * (s)}}\right) - \rho s^2 sin\left(ih\sqrt{\frac{\rho s}{\eta\eta * (s)}}\right)\left(ih\sqrt{\frac{\rho s}{\eta\eta^*(s)}}\right)_s' =$$

$$-\rho s^2(-1)^n\left(ih\sqrt{\frac{\rho s}{\eta\eta^*(s)}}\right)_s' = -\rho s^2(-1)^n\frac{ih}{\sqrt{\nu}}\left(\sqrt{\frac{s}{\eta^*(s)}}\right)_s'. \tag{18}$$

where: $\nu = \frac{\eta}{\rho}$. Derivative $\left(\sqrt{\frac{s}{\eta^*(s)}}\right)_s'$ from formula (18) is calculated as:

$$\left(\sqrt{\frac{s}{\eta^*(s)}}\right)_s' = \frac{1}{2\left(\sqrt{\frac{s}{\eta^*(s)}}\right)}\left(\frac{s}{\eta^*(s)}\right)_s' = \frac{1}{2\left(\sqrt{\frac{s}{\eta^*(s)}}\right)}\left(\frac{\eta^*(s)-s(\eta^*(s))_s'}{\eta^{*2}(s)}\right). \tag{19}$$

Since $\frac{ih}{\sqrt{\nu}}\sqrt{\frac{s}{\eta^*(s)}} = \frac{2n+1}{2}\pi$, therefore:

$$\left(\sqrt{\frac{s}{\eta^*(s)}}\right)_s' = \frac{ih}{(2n+1)\pi\sqrt{\nu}}\left(\frac{\eta^*(s)-s(\eta^*(s))_s'}{\eta^{*2}(s)}\right). \tag{20}$$

Considering that $\eta^*(s) = -\frac{4s}{(2n+1)^2\pi^2}\frac{h^2}{\nu}$, Eq. (20) takes the following form:

$$\left(\sqrt{\frac{s}{\eta^*(s)}}\right)_s' = \frac{ih}{(2n+1)\pi\sqrt{\nu}}\left(\frac{\eta^*(s) - s\left(\eta^*(s)\right)_s'}{\eta^{*2}(s)}\right) =$$

$$= \frac{ih}{(2n+1)\pi\sqrt{\nu}} \frac{(2n+1)^4\pi^4}{16s^2} \frac{\nu^2}{h^4}\left(\eta^*(s) - s\left(\eta^*(s)\right)_s'\right). \quad (21)$$

With the found derivatives (21) and (18), we find the formula for calculating the denominator (13):

$$F_2{}'(s) = -\rho s^2(-1)^n \frac{ih}{\sqrt{\nu}}\left(\sqrt{\frac{s}{\eta^*(s)}}\right)_s' =$$

$$= -\rho s^2(-1)^n \frac{ih}{\sqrt{\nu}} \frac{ih}{(2n+1)\pi\sqrt{\nu}} \frac{(2n+1)^4\pi^4}{16s^2} \frac{\nu^2}{h^4}\left(\eta^*(s) - s\left((\eta^*(s)\right)_s'\right)$$

$$=$$

$$= \rho(-1)^n \frac{(2n+1)^3\pi^3}{16} \frac{\nu}{h^2}\left(\eta^*(s) - s\left((\eta^*(s)\right)_s'\right). \quad (22)$$

Instead of $\eta^*(s)$, substituting its value

$$\eta^*(s) = (X + Z\frac{1}{1+s\lambda})\eta^*{}'(s) = \frac{-\lambda Z}{(1+s\lambda)^2}$$

$$\eta^*(s) - s\eta^*{}'(s) = (X + Z\frac{1}{1+s\lambda}) - \frac{-s\lambda Z}{(1+s\lambda)^2} =$$

$$= \frac{1 + 2\lambda s + \lambda^2 s^2 X}{(1+s\lambda)^2}$$

in (22) and considering that $s = -\frac{\nu}{h^2}\bar{s}, De = \frac{\lambda\nu}{h^2}$, we obtain

$$F_2{}'(\bar{s}) = \rho(-1)^n \frac{(2n+1)^3\pi^3}{16} \frac{\nu}{h^2}\left(\eta^*(s) - s\left((\eta^*(s)\right)_s'\right) =$$

$$= (-1)^n \frac{(2n+1)^3\pi^3}{16} \frac{\eta}{h^2} \frac{1 - 2De\bar{s} + De^2\bar{s}^2 X}{(1-sDe)^2}. \quad (23)$$

Substituting $F_1(\bar{s})$ and $F_2{}'(\bar{s})$ from (17) and (23) into (13), and replacing $\bar{s}$ with $\bar{s}_{in}$, we obtain the final values for C_{in}:

$$C_{in} = \frac{F_1(s_{in})}{F_2'(s_{in})} = \sum_{n=1}^{\infty}\sum_{i=1}^{2} \frac{\left(-\frac{dp}{dx}\right)\left(-cos\left(\frac{(2n+1)}{2}\pi\frac{y}{h}\right)e^{-\frac{\nu}{h^2}\bar{s}_{in}t}\right)}{(-1)^{n+1}\frac{(2n+1)^3\pi^3}{16}\frac{\eta}{h^2}\frac{1 - 2De\bar{s}_{in} + De^2\bar{s}_{in}{}^2 X}{(1-s_{in}De)^2}} =$$

$$= \frac{16h^2}{\eta}\left(-\frac{\partial p}{\partial x}\right)\sum_{n=1}^{\infty}\sum_{i=1}^{2} \frac{(-1)^n cos\left(\frac{(2n+1)}{2}\pi\frac{y}{h}\right)e^{-\frac{\nu}{h^2}\bar{s}_{in}t}}{(2n+1)^3\pi^3\frac{1 - 2De\bar{s}_{in} + De^2\bar{s}_{in}{}^2 X}{(1-s_{in}De)^2}}.$$

Summing up C_o and C_{in} and substituting into (11), Equation (3) has a solution that has the following form:

$$u(y,t) = \frac{h^2}{2\eta}\left(-\frac{dp(x)}{dx}\right)\left[\left(1 - \frac{y^2}{h^2}\right) + 32\sum_{n=1}^{\infty}\sum_{i=1}^{2} \frac{(-1)^n cos\left(\left(\frac{2n+1}{2}\right)\pi\frac{y}{h}\right)e^{-\frac{\nu}{h^2}\bar{s}_{in}t}}{(2n+1)^3\pi^3\frac{1 - 2De\bar{s}_{in} + De^2\bar{s}_{in}{}^2 X}{(1-s_{in}De)^2}}\right. \quad (24)$$

$$\frac{u(0,t)}{u_0} = 1 + 32\sum_{n=1}^{\infty}\sum_{i=1}^{2} \frac{(-1)^n e^{-\frac{\nu}{h^2}\bar{s}_{in}t}}{(2n+1)^3\pi^3\frac{1 - 2De\bar{s}_{in} + De^2\bar{s}_{in}{}^2 X}{(1-\bar{s}_{in}De)^2}}. \quad (25)$$

Here $u_0 = \frac{h^2}{2\eta}\left(-\frac{dp(x)}{dx}\right)$.

Expression (25) shows that the velocity distribution becomes parabolic as it gets closer to infinity.

$$u(y,t) = \frac{h^2}{2\eta}\left(-\frac{dp(x)}{dx}\right)\left[\left(1-\frac{y^2}{h^2}\right)\right] \tag{26}$$

Thus, the solution to the non-stationary motion problem when it approaches infinity yields the solution to the stationary fluid flow between parallel walls problem.

3 Results and Discussion

Numerical computations were performed to establish steady-state non-stationary processes with hydrodynamic properties during the non-stationary flow of a viscoelastic fluid, utilizing the obtained formulas (24) and (25). We initially investigate the Newtonian fluid in order to make comparisons between it and the steady-state viscoelastic fluid easier. The Newtonian fluid computation formulas are derived from (24) and (25), and for $\lambda = 0, \eta^*(s) = 1,\ X = 1,\ Z = 0$, The transcendental equation's solution in this instance takes the following form.

$$cos\left(i\sqrt{\frac{\rho s}{\eta}}h\right) = 0, \left(i\sqrt{\frac{\rho s}{\eta}}h\right) = \frac{2n+1}{2}\pi, s = -\frac{\nu}{h^2}\bar{s}, \bar{s} = \frac{(2n+1)^2}{4}\pi^2 \tag{27}$$

Using these expressions from formulas (24) and (25), calculation formulas to study Newtonian fluid can be obtained in the following form:

$$u(y,t) = \frac{h^2}{2\eta}\left(-\frac{dp(x)}{dx}\right)\left[\left(1-\frac{y^2}{h^2}\right) + 32\sum_{n=1}^{\infty}\frac{(-1)^n}{(2n+1)^3\pi^3}cos\left(\left(\frac{2n+1}{2}\right)\pi\frac{y}{h}\right)e^{-\frac{\nu}{h^2}\frac{(2n+1)^2}{4}\pi^2 t}\right] \tag{28}$$

$$\frac{u(0,t)}{u_{0\max}} = 1 + 32\sum_{n=1}^{\infty}\frac{(-1)^n}{(2n+1)^3\pi^3}e^{-\frac{\nu}{h^2}\frac{(2n+1)^2}{4}\pi^2 t} \tag{29}$$

Numerical computations were carried out using formula (29), as seen in Fig. 1, to show how the ratio of the maximum velocity to the maximum velocity of a stationary flow changes with time. It is evident that the relative maximum velocity of a Newtonian fluid in a non-stationary flow increases monotonically with time to the value of a stationary flow.

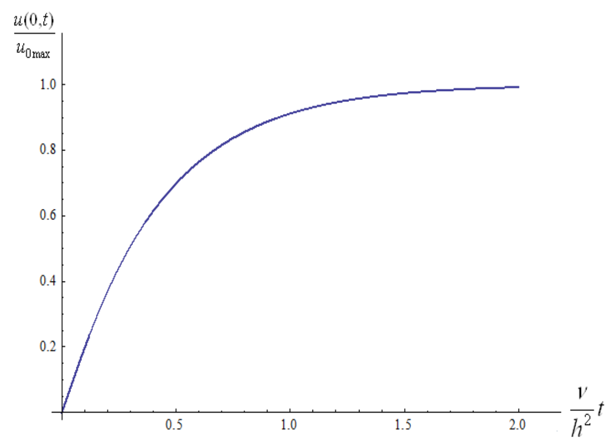

Fig. 1. Variation in the maximum velocity to stationary profile maximum velocity ratio over time in an unsteady Newtonian fluid flow

Numerous literary sources [7-12] provide information regarding the method by which a Newtonian fluid moves from a non-stationary to a stationary flow regime. Nevertheless, not enough research has been done on the process by which viscoelastic fluids go from an unstable to a stationary flow. The unsteady flow of a viscoelastic fluid in annular pipes is the subject of references [15, 16]. The finite difference approach is used to solve these problems. An investigation of the issue resolved with the generalized two-fluid Maxwell model is shown below.

We employ formulas (24) and (25), to do this. One of the physical characteristics of a viscoelastic fluid flow is that, after reaching its maximum velocity initially, the flow enters a stage of stagnant flow and monotonic reduction. The Maxwell model is used to examine the process of a viscoelastic fluid changing from an unstable to a stationary condition in a flat channel, based on formulas (24) and (25). In this instance, roots entering formulae (24) and (25) yield the solution to the quadratic equation (16).

There are two roots identified for the quadratic equation (16): real different, real equal, and complex conjugate.

$$s_{1n} = \frac{1+XDea_0^2+\sqrt{1-2Dea_0^2(X-2)+X^2De^2a_0^4}}{2De}, \tag{30}$$

$$s_{2n} = \frac{1+XDea_0^2-\sqrt{1-2Dea_0^2(X-2)+X^2De^2a_0^4}}{2De} \tag{31}$$

For a quadratic equation to have real roots, the discriminant in formulas (30) and (31) $(1-2Dea_0^2(X-2)+X^2De^2a_0^4\ )$ Needs to be at least as high as zero.In this case, the roots are real, so the solutions to equations (24) and (25) are presented in the following form:

$$u(y,t) = \frac{h^2}{2\eta}\left(-\frac{dp(x)}{dx}\right)\left[\left(1-\frac{y^2}{h^2}\right) + 32\sum_{n=0}^{\infty}\sum_{i=1}^{2}\frac{(-1)^{n+1}\cos\left(\left(\frac{2n+1}{2}\right)\pi\frac{y}{h}\right)e^{-\frac{\nu}{h^2}\bar{s}_{in}t}}{(2n+1)^3\pi^3\frac{1-2De\bar{s}_{in}+De^2\bar{s}_{in}{}^2X}{(1-s_{in}De)^2}}\right. \tag{32}$$

$$\frac{u(0,t)}{u_0} = 1 + 32\sum_{n=0}^{\infty}\sum_{i=1}^{2}\frac{(-1)^{n+1}e^{-\frac{\nu}{h^2}\bar{s}_{in}t}}{(2n+1)^3\pi^3\frac{1-2De\bar{s}_{in}+De^2\bar{s}_{in}{}^2X}{(1-\bar{s}_{in}De)^2}}. \tag{33}$$

In this case, solutions to (32) and (33) will be the same as solutions to (24) and (25). Analysis of formulas (32) and (33) is given in Fig. 2.

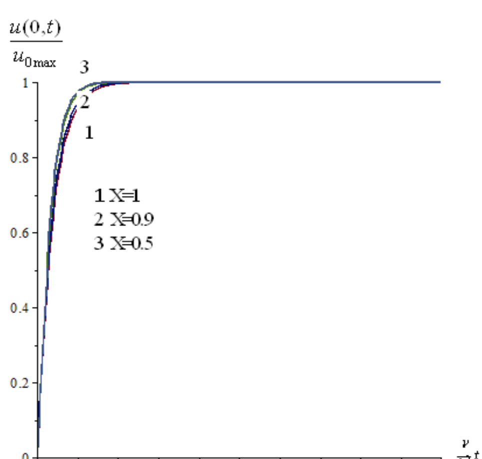

Fig. 2. Variation in the ratio of the maximum velocity to the maximum velocity of a stationary profile over time in an unstable viscoelastic fluid flow (for varying values of the Newtonian fluid concentration and Deborah number)

From Figure. 2, it is evident that in this instance, the non-stationarity processes in the flow of an elastic-viscous fluid and the non-stationarity processes in a Newtonian fluid are virtually equivalent. In this instance, the method of stabilizing the non-stationary flow of a Newtonian fluid can be used in place of the erratic flow of an elastic-viscous fluid. Now consider the situation when complex conjugate roots make up the roots of quadratic equation (16). When the discriminant of equation (16) is less than zero, this instance is observed. In this instance, the quadratic equation's solution is found to be:

$$s_{1n} = \frac{1+XDea_0^2+i\sqrt{2Dea_0^2(2-X)-X^2De^2a_0^4-1}}{2De} = a+bi \tag{34}$$

$$s_{2n} = \frac{1+XDea_0^2-i\sqrt{2Dea_0^2(2-X)-X^2De^2a_0^4-1}}{2De} = a-bi \tag{35}$$

Here $a = \frac{1-XDea_0^2}{2De}, b = \frac{\sqrt{2Dea_0^2(2-X)-X^2De^2a_0^4-1}}{2De}, a_0 = \frac{2n+1}{2}\pi, De = \frac{\lambda\nu}{h^2},\ s_{1n} = a + bi, s_{2n} = a - bi$

Then solutions to (24) and (25) have the following form:

$$u(y,t) = \frac{h^2}{2\eta}\left(-\frac{dp(x)}{dx}\right)\left[\left(1-\frac{y^2}{h^2}\right)+\right.$$

$$\left.32\sum_{n=0}^{\infty}\frac{(-1)^{n+1}\cos\left(\left(\frac{2n+1}{2}\right)\pi\frac{y}{h}\right)2e^{-\frac{\nu}{h^2}a_nt}}{(2n+1)^3\pi^3(M_2^2+N_2^2)}\left(M_3\cos b_n\frac{\nu}{h^2}t + N_3\sin b_n\frac{\nu}{h^2}t\right)\right. \tag{36}$$

$$\frac{u(0,t)}{u_0} = 1 + 32\sum_{n=0}^{\infty}\frac{2(-1)^{n+1}e^{-\frac{\nu}{h^2}a_nt}}{(2n+1)^3\pi^3(M_2^2+N_2^2)}\left(M_3\cos b_n\frac{\nu}{h^2}t + N_3\sin b_n\frac{\nu}{h^2}t\right). \tag{37}$$

Here

$$M_1 = 1-2a_nDe+a_n^2De^2-b_n^2, N_1 = 2a_nb_n-2b_nDe$$
$$M_2 = 1-2a_nDe+a_n^2De^2X-De^2b_n^2X, N_2 = 2a_nb_nDe^2X-2b_nDe$$
$$M_3 = M_1M_2+N_1N_2, N_3 = -(M_1N_2-M_2N_1)$$

We examine the numerically calculated unsteady flow of an elastic-viscous fluid where the solutions to equation (16) are composed of complex conjugate roots using formula (37). Figures 3-6 (for the Deborah numbers and various values of the Newtonian fluid concentration) illustrate the change in time in the ratio of the maximum velocity to the maximum velocity of a stationary profile during an unsteady flow of a viscoelastic fluid.It is evident from the pictures that, in contrast to a Newtonian fluid, the transition from an unstable to a stationary state (based on the generalized Maxwell model of a viscoelastic fluid) is wave-like. The Maxwell model of a viscoelastic fluid has a transition time that is several times longer than the Newtonian fluid models, as Figures 3-6 demonstrate. In Figure 1, for instance, it is three times longer; in Figure 2, it is four times longer; in Figure 5, it is 3.5 times longer; and in Figure 6, it is 4.5 times longer.

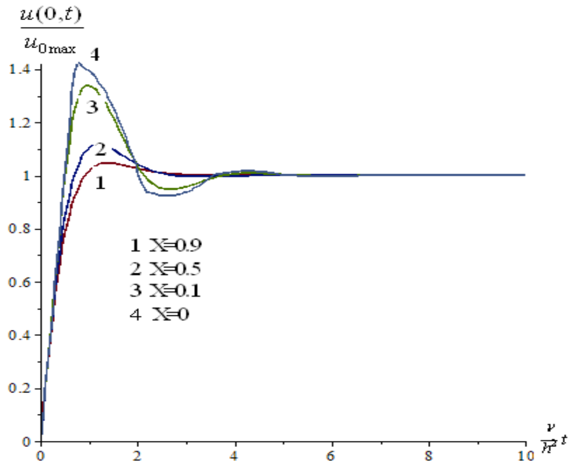

Fig. 3. Variation in the maximum velocity to the maximum velocity of a stationary profile over time in an unstable viscoelastic fluid flow (for varying Newtonian fluid concentration levels and Deborah numbers)

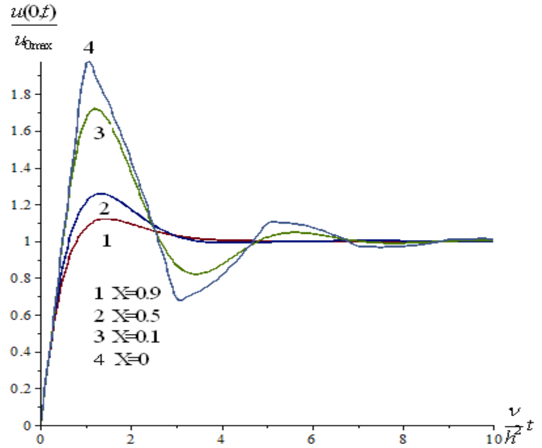

Fig. 4. Variation in the maximum velocity to the maximum velocity of a stationary profile over time in an unstable viscoelastic fluid flow (for varying Newtonian fluid concentration levels and Deborah numbers)

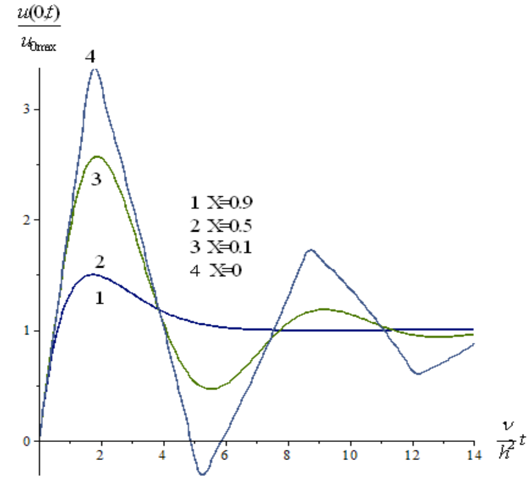

Fig. 5. Variation in the maximum velocity to the maximum velocity of a stationary profile over time in an unstable viscoelastic fluid flow (for varying Newtonian fluid concentration levels and Deborah numbers)

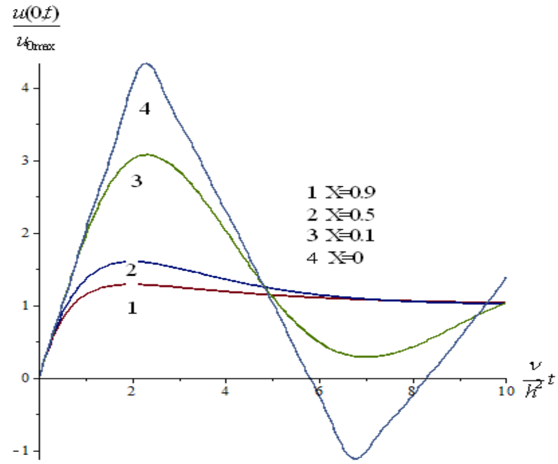

Fig. 6. Variation in the maximum velocity to the maximum velocity of a stationary profile over time in an unstable viscoelastic fluid flow (for varying Newtonian fluid concentration levels and Deborah numbers)

The primary cause of the abrupt increase in hydrodynamic quantities during the transition of an elastic-viscous fluid can be assumed to be the inertial force taken into account in the Maxwell model. It is evident that, once the inertial force is removed, the fluid behaves exactly like a Newtonian fluid. The Deborah number, or relaxation, in this case explains the inertial force's effect. Figures 5 and 6 illustrate how the increase in the Deborah number during the transition process surpasses the ratio of the maximum velocity to the maximum velocity of the stationary profile of a viscoelastic fluid by 4.5–5 times when compared to the maximum velocity of a Newtonian fluid. It is evident from Figures 3–6 that the uneven motion of the mixture can, in a way, stabilize a viscoelastic fluid that is created by combining a Newtonian fluid with unsteady flows of viscoelastic fluids. In this instance, the characteristics can be normalized by an instantaneous maximum rise in the relative maximum velocity due to an increase in the Newtonian fluid concentration. In technical and technological processes, ensuring the implementation of this function is crucial to preventing malfunctions and failures.

4 Conclusion

The problem of unsteady flow of an elastic-viscous fluid in a flat channel under the effect of a constant pressure gradient was solved using the generalized Maxwell model. The distribution of the fluid flow rate and velocity profile in an unsteady flow of viscoelastic fluid were calculated using the derived formulas. The methods by which the properties of an elastic-viscous fluid in a flat channel change from an unstable to a stationary state were examined using the formulas that were found. Considering the analysis's conclusions. It was demonstrated that transient processes in an elastic-viscous fluid that rely on the Debord number which establishes the fluid's elasticity property differ significantly from transient processes in a Newtonian fluid. It was found that at small values of the Deborah number, the processes of transitioning the properties of an elastic-viscous fluid from an unstable to a stationary state are essentially the same as those of a Newtonian fluid. It was discovered that the process of an elastic-viscous fluid changing from an unstable to a stationary state is wave-like at large values of the Deborah number. The transition time is several times longer than the transition time of a Newtonian fluid, in contrast to the transition process itself. Additionally, it was shown that during the transition, disturbed processes can emerge. In a sense, the perturbed processes in viscoelastic fluid that occur in unsteady flows can be stabilized with the addition of Newtonian fluid. This demonstrates how a Newtonian fluid's disturbed properties can be normalized by an instantaneous maximum rise in the relative maximum velocity brought on by an increase in fluid concentration. In technical and technological procedures, this property's application is crucial for averting malfunctions or breakdowns.

References

1. Mirzajanzade A.Kh., Karaev A.K., Shirinzade S.A. Hydraulics in drilling and cementing oil and gas wells. M.: Nedra, 1977.
2. Ametov I.M., Baidikov Yu.N., Ruzin L.M. etc. Extraction of heavy and high-viscosity liquids. M.: Nedra, 1985.
3. Gromeka I.S. On the theory of fluid motion in narrow cylindrical tubes. Collection Op. – M., 1952. – p. 149-171.
4. Gromeka I.S. On the propagation velocity of fluid wave motion in elastic pipes. Collection op. – M., 1952. – p. 172-183.13.
5. Loytsyansky L.G. Fluid and gas mechanics. – M.: Bustard, 2003.-840 p.8.
6. Faizullaev D.F., Navruzov K. Hydrodynamics of pulsating flows, Tashkent, “Fan”, 1986. – 192 p.
7. Kolesnichenko V.I., Sharifulin A.N. Introduction to incompressible fluid mechanics. – Perm, Ed. Perm National Research Polytechnic University, 2019. – 127 p.
8. Slezkin N.A. Dynamics of a viscous incompressible fluid. – M.: Gostekhizdat, 1956. – 520 p.
9. Targ S.M. Main problems of the theory of laminar flows. – M.: Gostekhizdat, 1954. – 420 p.
10. Schlichting G. Theory of the boundary layer. – M.: Nauka, 1974. – 712 p.

11. Hassan, A. Abu-EL. and El-Maghawry Unsteady axial viscoelastic pipe flows of an Oldroyd B fluid in: Rheology-New concepts, Applications and Methods, EA by Durairaj R., Published by In Tech., 2013, ch. 6, p.91-106
12. Navruzov K., Khakberdiev Zh.B. Dynamics of non-Newtonian fluids. – Tashkent: Fan", 2000. – 246 p.
13. Navruzov K., Sharipova Sh. B. Tangential Shear Stress in an Oscillatory Flow of a Viscoelastic incompressible fluid in a flat Channel //Fluid Dynamics, 2023, vol. 58, No 3. P. 360-370.
14. Navruzov K., Fayziev R.A., Mirzoev A.A. Sharipova Sh. B. Tangential Shear Stress in an Oscillatory Flow of a Viscoelastic Fluid in a Flat Channel // Lecture Notes in Computer Science (including subseries Lecture Notes in Artificial Intelligence and Lecture Notes in Bioinformatics), 2023. P.1-14.
15. Shulman Z.P., Khusid B.M. Non-stationary processes of convective transport in hereditary media. – Minsk, 1983. – 256 p.
16. Shulman Z.P., Khusid B.M. Phonological and microstructural theories of hereditary fluids, // Institute of Heat and Mass Transfer of the Academy of Sciences of Belarus. Prepr., 1983, No. 4. – 50 p.
17. Casanellas L., Ortin J. Laminar oscillatory flow of Maxwell and Oldroyd-B fluids// J. Non-Newtonian Fluid. Mechanics. 166. 2011. P. 1315-1326.
18. Ding Z., Jian Y. Electro-kinetic oscillatory flow and energy micro-channels: a linear analysis // J. Fluid. Mech. 2021. vol. 919. A20. P.1-31.
19. Astarita G., Marrucci G. Fundamentals of hydromechanics of non-Newtonian fluids. M.: Mir. 1978. 309 p.
20. Navruzov K., Rajabov S., Ashirov M. Mathematical modeling of hydrodynamic resistance an oscillatory flow of a viscoelastic fluid // E3S Web of conferences 401. 02026/ 2023 (CONMECHYDREO-2023). P.1-10.
21. Navruzov K., Turaev M., Shukurov Z. Pulsating flows of viscous fluid in channel for given harmonic fluctuation of flow rate // E3S Web of conferences 401. 02010/ 2023 (CONMECHYDREO-2023). P.1-8.
22. Daliev, S., Karshiev D., Islamov Y. Mathematical modeling of salt concentration change process in two-layer aqueous media. E3S Web of Conferences. 2023, 401, 02009 DOI.ORG/10.1051/E3SCONF/202340102009
23. Daliev S., Ravshanov N. Numerical and mathematical modeling of changes in groundwater levels in two-layer media. ICISCT 2022, DOI: 10.1109/ICISCT55600.2022.10146793